

Shape Feature Analysis of Concealed Objects with Passive Millimeter Wave Imaging

Seokwon Yeom^{*}, Dong-Su Lee, and Jung-Young Son

Abstract—Millimeter wave (MMW) imaging has found rapid adoption in security applications such as concealed object detection under clothing. However, the imaging quality is often degraded due to resolution limit and low signal level. This study addresses shape feature analysis following concealed object detection. The object region is extracted by multi-level segmentation. Shape features are composed of several descriptors which are object area, perimeter, major and minor axes of the basic rectangle, rectangularity, compactness, and eccentricity. In the experiments, three objects (gun, hand ax, and plastic bottle containing liquid skin aid) concealed under clothing are captured by the passive MMW imaging system. The extracted shape features are compared with the true features from the object model showing good accuracy.

1. INTRODUCTION

Millimeter wave (MMW) imaging has been widely adopted in security and military applications [1–6]. Passive MMW imaging can generate interpretable images under low visibility conditions such as fog, rain, dust, and smoke. One of the rapidly adopted applications is concealed weapon detection. The imaging of the concealed object is accomplished by radiometric temperature differences. The effective radiometric temperature depends on the emissivity and reflectivity as well as physical temperatures [1]. Unfortunately, the image quality in such applications is often degraded by diffraction limit and low signal-to-noise ratio (SNR).

There have been researches on the automatic detection of concealed objects [7–14]. The multi-level thresholding was addressed to detect the contours of the concealed objects from Terahertz images [7]. The image segmentation using the Gaussian mixture model (GMM) has been researched on the metallic object detection [8]. Multi-level segmentation has been proposed to cluster pixels adopting the expectation and maximization (EM) algorithm [9, 10]. Object identification has been performed using the radiation characteristics of a target in a close range [11]. Studies on concealed weapon identification and navigation were presented in [12]. Shape-based object matching and recognition can be found in [13]. In [14], the classification of two metallic objects was addressed with geometric features.

Shape feature extraction plays an important role in object retrieval, recognition and classification, and alignment and registration [15]. Shape features are required to be invariant to translation, rotation, and scale [16, 17]. In the paper, we address the shape feature analysis following the concealed object segmentation. Several shape features such as object area, perimeter, major and minor axes of the basic rectangle, rectangularity, compactness, and eccentricity are chosen to identify the hidden object. A person hiding a metal or a non-metallic object (gun, hand ax, or plastic bottle containing liquid skin aid) under clothing is captured by passive MMW imaging. The imaging system operates on 3 mm wavelength regime with a 0.5 m dish antenna. The shape features are extracted from the concealed

Received 10 August 2015, Accepted 9 November 2015, Scheduled 2 December 2015

^{*} Corresponding author: Seokwon Yeom (yeom@daegu.ac.kr).

The authors are with Division of Computer and Communication Engineering, Daegu University, Gyeongsan, Gyeongbuk 712-714, Korea.

object region, which is segmented by the multi-level segmentation [9, 10]. True shape features are obtained from the binary object model built on the actual object size. The extracted shape features from the passive MMW images are compared with the true features showing good accuracy around 87–92%.

This paper is organized as follows. In Sections 2 and 3, brief descriptions of the passive MMW imaging system and the multi-level segmentation are respectively presented. The shape feature analysis is discussed in Section 4. In Section 5, the experimental results are presented, and the conclusion follows in Section 6.

2. PASSIVE MILLIMETER WAVE IMAGING SYSTEM

Our passive MMW imaging system is equipped with a Cassegrain dish antenna with a diameter (D) of 0.5 m as shown in Figure 1(a) [10]. A feed horn antenna is installed at the focal plane of the dish antenna receiving the regime of 3 mm wavelength (λ). The angular resolution is around 0.42° according to the Rayleigh criterion when λ is 3 mm and D is 0.5 m. The receiver channel connected to the feed horn antenna is composed of a Dicke modulator, a dielectric wave guide, three monolithic microwave integrated circuit (MMIC) amplifiers, and a Schottky diode detector. The incoming electromagnetic wave is focused on the feed horn antenna, thus images are acquired by mechanical scanning of the dish antenna and the receiver. The scanning motors rotate both the antenna and the receiver in vertical and horizontal directions with a constant angular increment for raster scanning. Figure 1(b) demonstrates the scanning process for pixel formation where l is the distance to the imaging plane and α is the angular increment per step. A pixel pitch is approximately $2\alpha l$ since each pixel is obtained by averaging the adjacent values, which are obtained with a fixed scanning angle in vertical and horizontal directions. The feed antenna is scanned on the convex trail, but the imaging plane is approximated to be flat because the distance is much larger than the image size. Figure 1(c) is the block diagram of the signal flow.

3. CONCEALED OBJECT SEGMENTATION

The multi-level segmentation comprises global and local segmentations. The global segmentation separates a person's body area from the background. The local segmentation concerns only the inside of the body area in order to separate the object from the body. Figure 2 shows the block diagram of the multi-level segmentation.

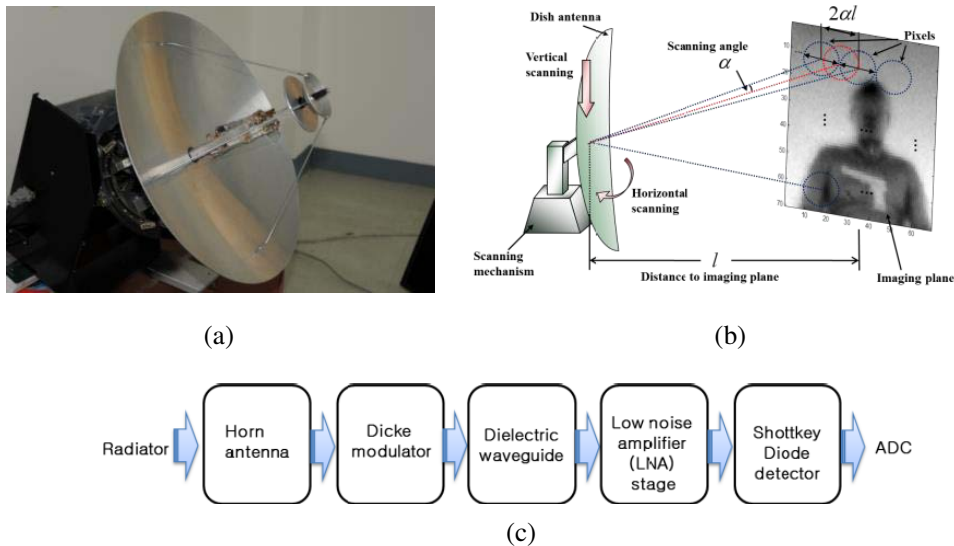


Figure 1. (a) Passive MMW imaging system, (b) pixel formation via scanning process, (c) signal flow.

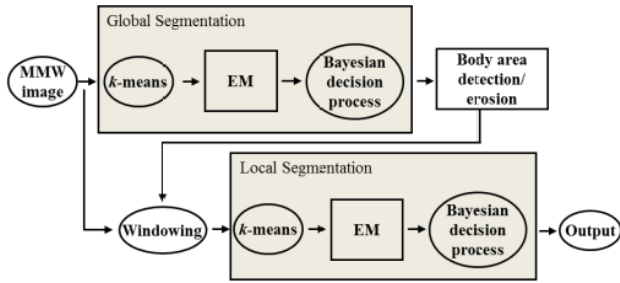


Figure 2. Block diagram of the multi-level segmentation.

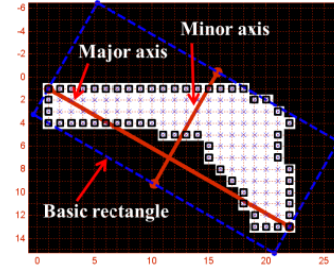


Figure 3. Shape features of a gun.

This multi-level segmentation adopts k -means clustering for the GMM parameter initialization. The k -means algorithm is an unsupervised learning method to compose a number of clusters without any prior information [18]. The initial centroids of the clusters are set either by the split from a centroid or the randomly selected. In the experiments, the initialization is chosen when better result is provided. Three parameters (mean, variance, and weight) of the GMM distribution are initiated by the k -means algorithm. The EM method is an iterative solution for the maximum likelihood estimation of the GMM parameters [19]. The first Bayesian decision rule is followed by body area detection, which fills up any segmented area inside the body. The morphological erosion process estimates the accurate contour of the body area. The second level EM followed by the Bayesian decision rule segments the concealed object in the body area. More detailed procedures of the multi-level segmentation are presented in [9, 10]

4. SHAPE FEATURE ANALYSIS OF CONCEALED OBJECTS

Several shape features are employed to identify hidden objects. They are area (A), perimeter (T), major axis (w), and minor axis (h) of the basic rectangle, rectangularity (r), compactness (c), and eccentricity (e). Area is obtained by the number of pixels belonging to the object. Perimeter is the number of pixels composing the object boundary. The major axis represents the distance between two extreme points on the boundary. The minor axis is the line perpendicular to the major axis.

Figure 3 shows the shape descriptors of the gun model. Area is the number of pixels marked by “ \times ” and perimeter is marked by “ \square ”. The major and minor axes compose each side of the basic rectangle, which is the smallest rectangle that bounds the object. Rectangularity is defined as

$$r = \frac{A}{A_R} \tag{1}$$

where A_R is the area of the basic rectangle. Rectangularity shows how rectangular an object is. For example, it is one when the object is a rectangle. Circularity representing the compactness of the object is defined as

$$c = \frac{4\pi A}{T^2} \tag{2}$$

It becomes one if the object is a circle. The following equation defines the eccentricity:

$$e = \sqrt{1 - \left(\frac{h}{w}\right)^2} \tag{3}$$

which is zero for a circle and between zero and one for ellipses.

5. EXPERIMENTAL RESULTS

A person who hides a metallic (gun or hand ax) or a non-metallic (plastic bottle containing liquid) object is captured by the passive MMW imaging system [20]. Figure 4(a) shows the actual size of

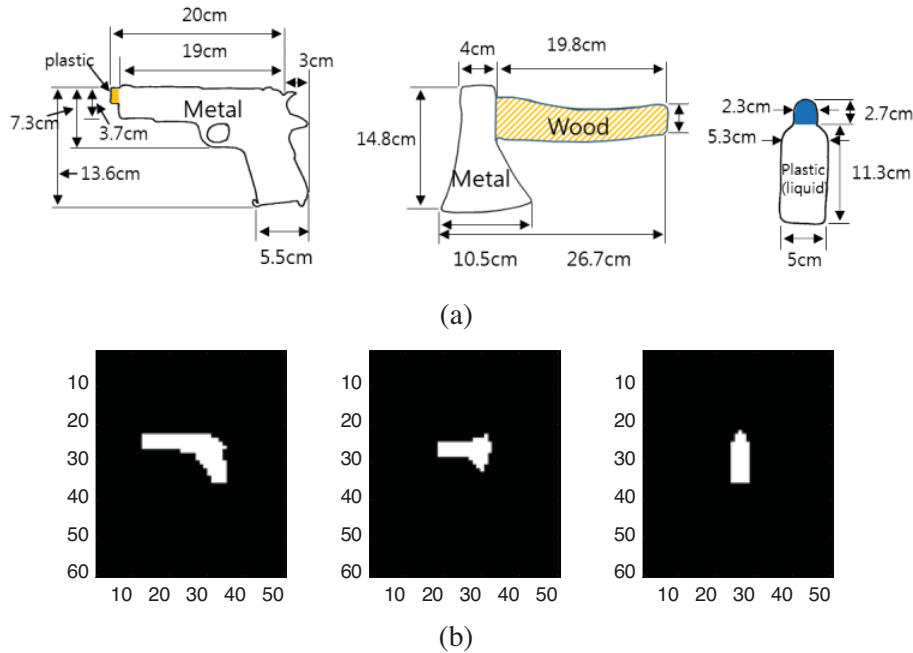


Figure 4. (a) Actual object size, (b) binary model.

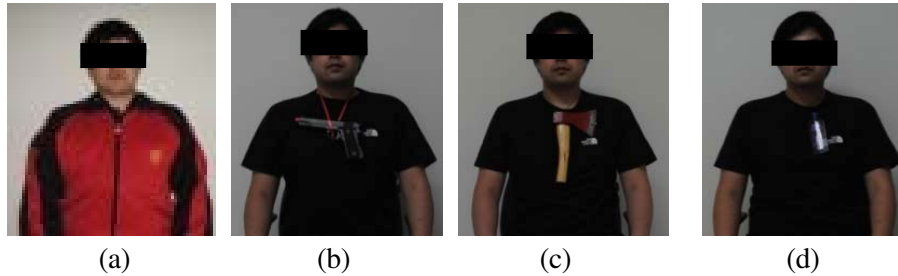


Figure 5. (a) A person hiding the object, demonstration of (b) gun, (c) hand ax, (d) plastic bottle containing liquid.

the objects. Figure 4(b) shows the binary models of Figure 4(a). The maximum sizes of the binary model for gun, hand ax, and plastic bottle are 22×13 , 14×10 , and 5×14 pixels, respectively. Thus, the pixel pitch in the binary object model corresponds to 1 cm. All of the passive MMW images are acquired when the person wears a sport training shirt to conceal the object as shown in Figure 5(a). Figures 5(b)–5(d) are presented only for demonstrating the objects attached to the person. The person faces the antenna 1.4 m away from the system. The scanning angle and the integrating time are set at 0.2° (≈ 0.0035 rad) and 60 msec, respectively. The images are acquired indoors during daytime without any illumination. The room temperature is around 22°C . The image size is 69×70 pixels. The metal, liquid in plastic, and wood (hand ax grip) are clearly visible as shown in Figures 6(a)–6(c).

Figure 7(a) is the global segmentation result of Figure 6(a) where the Gaussian mixture distribution in Figure 7(b) is obtained. The Gaussian distributions approximate the histogram derived from Figure 6(a). The white area of Figure 7(a) corresponds to the right Gaussian (red line) and the black area to the left Gaussian distribution (blue line). The local segmentation concerns only the black area after filling up any white area inside the body. Figure 7(c) is the combined results of the global and local segmentation. The white area in Figure 7(c) corresponds to the right Gaussian (red line) while the grey part to the left Gaussian distribution (blue line) in Figure 7(d). Other passive MMW images are processed the same way as shown in the Figures 8 and 9. It is noted that the plastic bottle with

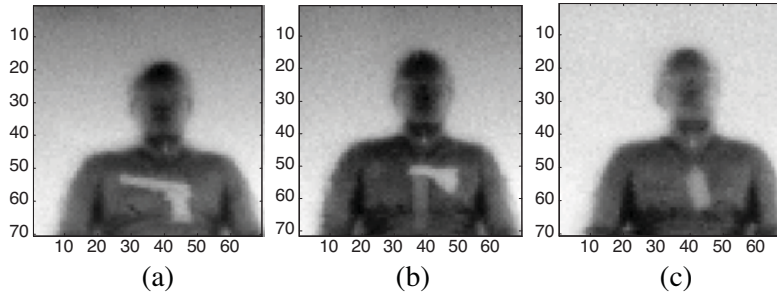


Figure 6. Passive MMW images of a person hiding, (a) gun, (b) hand ax, (c) plastic bottle containing liquid.

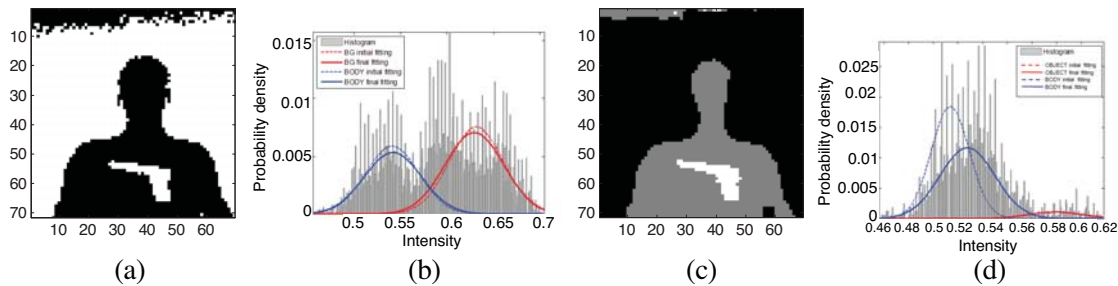


Figure 7. Gun, (a) global segmentation, (b) GMM fitting of global segmentation, (c) local segmentation, (d) GMM fitting of local segmentation.

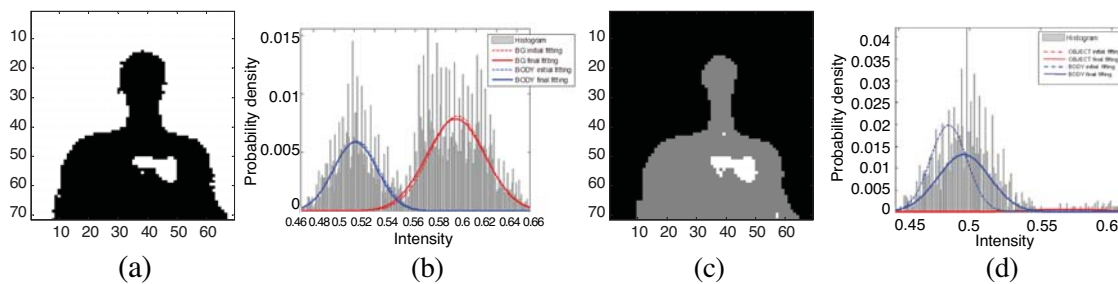


Figure 8. Hand ax, (a) global segmentation, (b) GMM fitting of global segmentation, (c) local segmentation, (d) GMM fitting of local segmentation.

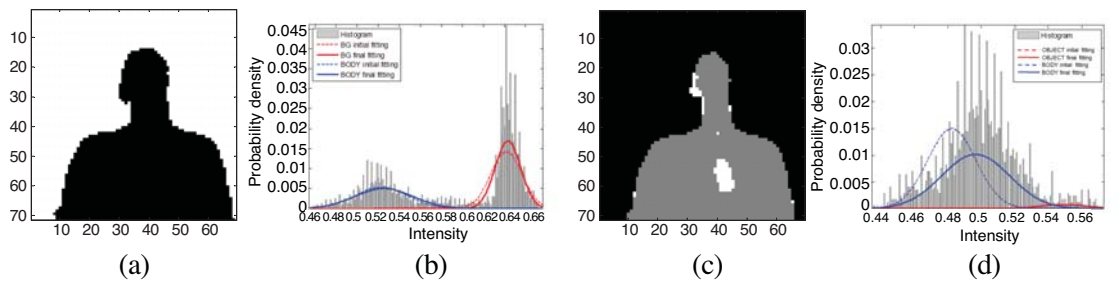


Figure 9. Plastic container with liquid, (a) global segmentation, (b) GMM fitting of global segmentation, (c) local segmentation, (d) GMM fitting of local segmentation.

liquid is not segmented during the global segmentation as shown in Figure 9(a).

Table 1 compares the true values of the shape features obtained from the binary models and the extracted features from the segmented objects. The relative errors are 0.112, 0.08, and 0.134 for gun, hand ax, and plastic bottle with liquid, respectively. Since one pixel pitch in the passive MMW images

Table 1. Shape feature analysis and comparison.

	Gun			Hand ax			Plastic bottle with liquid		
	Truth	MMW	Relative Error	Truth	MMW	Relative Error	Truth	MMW	Relative Error
Area (A)	137	100.84	0.264	72	74.91	0.040	62	50.9	0.179
Perimeter (T)	57	53.9	0.054	35	35.28	0.008	30	24.5	0.183
Major axis (w)	24.19	22.85	0.055	13.34	14.99	0.124	13.15	10.56	0.198
Minor axis (h)	11.16	10.42	0.067	9.29	8.08	0.131	5.47	5.28	0.036
Rectangularity (r)	0.508	0.424	0.165	0.584	0.619	0.060	0.861	0.914	0.062
Circularity (c)	0.530	0.436	0.177	0.739	0.756	0.023	0.866	1.066	0.230
Eccentricity (e)	0.887	0.890	0.003	0.717	0.843	0.176	0.909	0.866	0.047
Average			0.112			0.08			0.134

is slightly less than 1 cm ($2 \times 0.0035 \text{ rad} * 1.4 \text{ m} = 0.98 \text{ cm}$), area, perimeter and major and minor axes are compensated accordingly. The effective radiometric temperature highly depends on emissivity and reflectivity as well as the object and the ambient temperatures [1]. The emissivity of the liquid in the plastic bottle is closer to the body than other objects, which brings poor shape feature extraction following blurred object acquisition. The gunpoint has a narrow shape causing much error in estimating the area feature.

6. CONCLUSIONS

In this study, we have conducted shape feature analysis following the concealed object detection. Several shape features are extracted from the passive MMW images. They are compared with true values showing good accuracy around 87–92%. It has been seen that the accuracy depends on the radiation properties and the shape of the object. The former affects the effective radiometric temperature, and the latter is limited by the spatial resolution of the system. To recognize a number of objects automatically, pattern recognition technique [19] with learning process will be required, which remains for future study.

ACKNOWLEDGMENT

This work was supported by the Daegu University research grant.

REFERENCES

1. Yujiri, L., M. Shoucri, and P. Moffa, "Passive millimeter-wave imaging," *IEEE Microwave Magazine*, Vol. 4, No. 3, 39–50, 2003.
2. Appleby, R. and R. N. Anderton, "Millimeter-wave and submillimeter-wave imaging for security and surveillance," *Proc. IEEE*, Vol. 95, No. 8, 1683–1690, 2007.
3. Chen, H.-M., S. Lee, R. M. Rao, M.-A. Slamani, and P. K. Varshney, "Imaging for concealed weapon detection: A tutorial overview of development in imaging sensors and processing," *IEEE Signal Processing Magazine*, Vol. 22, 52–61, 2005.
4. Kim, W.-G., N.-W. Moon, H.-K. Kim, and Y.-H. Kim, "Linear polarization sum imaging in passive millimeter-wave imaging system for target recognition," *Progress In Electromagnetics Research*, Vol. 136, 175–193, 2013.
5. Demirci, S., H. Cetinkaya, E. Yigit, C. Ozdemir, and A. A. Vertiy "A study on millimeter-wave imaging of concealed objects: Application using back-projection algorithm," *Progress In Electromagnetics Research*, Vol. 128, 457–477, 2012.

6. Sato, H., K. Sawaya, K. Mizuno, J. Uemura, M. Takeda, J. Takahashi, K. Yamada, K. Morichika, T. Hasegawa, H. Hirai, H. Nikura, T. Matsuzaki, S. Kato, and J. Nakada, "Passive millimeter-wave imaging for security and safety applications," *Proc. of SPIE*, Vol. 7671, 76710V, 2010.
7. Shen, X., C. R. Dietlein, E. Grossman, Z. Popovic, and F. G. Meyer, "Detection and segmentation of concealed objects in Terahertz images," *IEEE Trans. on Image Processing*, Vol. 17, No. 12, 2465–2475, 2008.
8. Haworth C. D., Y. De Saint-Pern, D. Clark, E. Trucco, and Y. R. Petillot, "Detection and tracking of multiple metallic objects in millimeter-wave images," *International Journal of Computer Vision*, Vol. 71, 183–196, 2007.
9. Yeom, S., D. Lee, J.-Y. Son, M. Jung, Y. Jang, S. Jung, and S. Lee, "Real-time outdoor concealed-object detection with passive millimeter wave imaging," *Opt. Express*, Vol. 19, No. 3, 2530–2536, 2011.
10. Yeom, S., D. Lee, and J.-Y. Son, "Multi-level segmentation of passive millimeter wave images for hidden object detection," *Optical Engineering*, Vol. 51, 091613, 2012.
11. Li, L. C., J. Y. Yang, G. L. Cui, Z. M. Jiang, and X. Zheng, "Method of passive MMW image detection and identification for close target," *J. Infrared, Millimeter Terahertz Waves*, Vol. 32, Nos. 102–115, 2011.
12. Jacobs, E. L. and O. Furrxi, "Target identification and navigation performance modeling of a passive millimeter wave imager," *Appl. Opt.*, Vol. 49, E94–E105, 2010.
13. Belongie S., J. Malik, and J. Puzicha "Shape matching and object recognition using shape contexts," *IEEE PAMI*, Vol. 24, 509–521, 2002.
14. Yeom, S., D. Lee, Y. Jang, M. Lee, and S. Jung, "Real-time outdoor concealed-object detection with passive millimeter wave imaging," *Opt. Express*, Vol. 20, No. 9, 9371–9381, 2012.
15. Gonzalez, R. C., *Digital Image Processing 2/E*, Prentice-Hall Inc., 2003.
16. Pitas, I., *Digital Image Processing Algorithms and Applications*, John Wiley & Sons, Inc., 2000.
17. Mingqiang, Y., K. Kidiyo1, and R. Joseph, *Pattern Recognition Techniques, Technology and Applications. Ch. 3: A Survey of Shape Feature Extraction Techniques*, InTech, 2008.
18. Gersho, A. and R. M. Gray, *Vector Quantization and Signal Compression*, Kluwer Academic Publishers, Boston, MA, 1992.
19. Bishop, C. M., *Neural Networks for Pattern Recognition*, Oxford, 1995.
20. Yeom, S., D. Lee, H. Lee, J. Son, and V. P. Gushin, "Vector clustering of passive millimeter wave images with linear polarization for concealed object detection," *Progress In Electromagnetics Research Letters*, Vol. 39, 169–180, 2013.